A real-time PCR-based method for determining the surface coverage of thiol-capped oligonucleotides bound onto gold nanoparticles

Eun-Young Kim[1,2], Jennifer Stanton[1], Rafael A. Vega[2,3], Kevin J. Kunstman[1], Chad A. Mirkin[2,3] and Steven M. Wolinsky[1,2,*]

[1]Department of Medicine, Feinberg School of Medicine, Northwestern University, Chicago, IL 60611, USA, [2]International Institute for Nanotechnology and [3]Department of Chemistry, Northwestern University, Evanston, IL 60208, USA

ABSTRACT

Here we report a real-time PCR-based method for determining the surface coverage of dithiol-capped oligonucleotides bound onto gold nanoparticles alone and in tandem with antibody. The detection of gold nanoparticle-bound DNA is accomplished by targeting the oligonucleotide with primer and probe binding sites, amplification of the oligonucleotide by PCR, and real-time measurement of the fluorescence emitted during the reaction. This method offers a wide dynamic range and is not dependant on the dissociation of the oligonucleotide strands from the gold nanoparticle surface; the fluorophore is not highly quenched by the gold nanoparticles in solution during fluorescence measurements. We show that this method and a fluorescence-based method give equivalent results for determining the surface coverage of oligonucleotides bound onto 13 or 30 nm gold nanoparticles alone and in tandem with antibody. Quantifying the surface coverage of immobilized oligonucleotides on metallic nanoparticle surfaces is important for optimizing the sensitivity of gold nanoparticle-based detection methods and for better understanding the interactions between thiol-functionalized oligonucleotides and gold nanoparticles.

INTRODUCTION

Determining the surface coverage, structure, and function of oligonucleotides immobilized onto a metal nanoparticle surface is important for both understanding the interactions between the two moieties and optimizing the sensitivity of metal nanoparticle-based methods for DNA and protein detection (1–6). These detection methods leverage the small label size, established conjugation chemistry, and the physical, chemical and electrical properties of metal nanoparticles (7–10). Two parameters that affect the magnitude of measurable change in these detection methods are the extent of surface modification of the metal nanoparticle and the accessibility of the complementary target DNA sequence to the surface-bound oligonucleotide (1,11–13). Knowledge of these parameters is important for achieving a balance between oligonucleotide surface coverage and hybridization efficiency.

Several techniques including electrochemistry, surface plasmon resonance spectroscopy, and fluorescence have been used to measure surface coverage of oligonucleotides bound to metallic nanoparticles and thin-film metallic surfaces (1,14,15). These measurements first require displacement of the oligonucleotides from the metal surface because of fluorescence quenching due to non-radiative energy transfer from the fluorophore to the metal (16). Normalized surface coverage is then back calculated from the measured quantity of oligonucleotides and from the estimated particle surface area. Although extremely useful, this assay is somewhat cumbersome and requires modification of the surface bound oligonucleotides by adding thiol and fluorophore functionalities (1). Therefore, the fluorophore assay focuses on a model system for the probes rather than the nanoparticle probes themselves, which do not typically have fluorophores.

Herein we report a real-time PCR-based method for determining the surface coverage of dithiol-capped oligonucleotides bound onto a gold nanoparticle surface. The detection of gold nanoparticle-bound DNA is accomplished by targeting the oligonucleotide with primer and probe binding sites, amplification of the DNA by PCR, and real-time measurement of the fluorescence emitted during the reaction (Figure 1). Unlike the existing methods for measuring surface coverage of oligonucleotides bound onto metallic surfaces, this method

*To whom correspondence should be addressed: Tel: +1 312 695 5067; Fax: +1 312 695 5088; Email: s-wolinsky@northwestern.edu
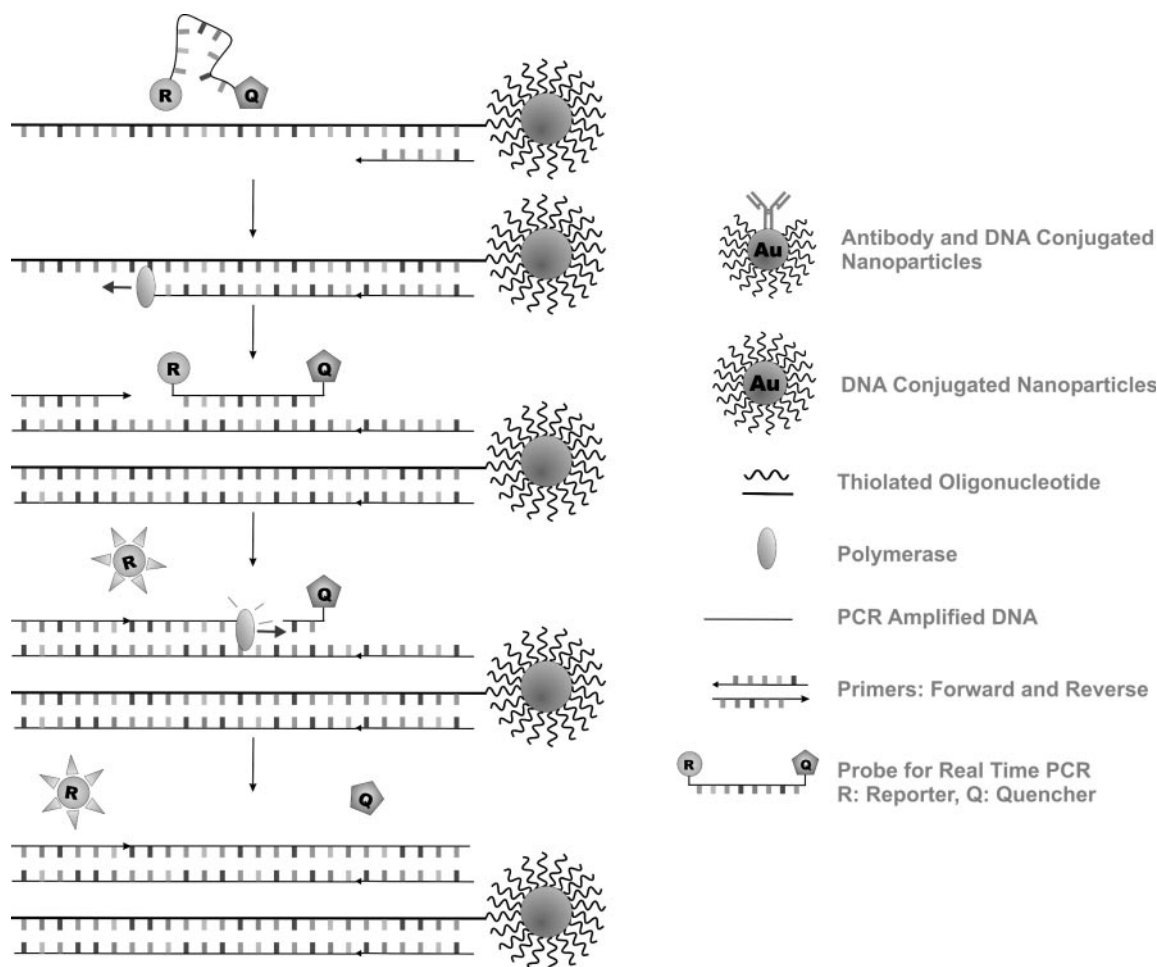
Figure 1. Real–time PCR-based method for determining the surface coverage of 5′-thiol oligonucleotides bound to gold nanoparticles.

does not require specific oligonucleotides that are different from the ones typically used in nanoparticle assays (i.e. fluorophore modification). Moreover, RT–PCR detection enables quantitative measurements of oligonucleotide surface coverage over a wide dynamic range and allows for the ability to work with a very low concentration of particles.

MATERIALS AND METHODS

DNA oligonucleotides

The DNA sequence for the bound thiol-capped oligonucleotide was selected from *Arabidopsis* database (http://genomics.msu.edu/plant_specific/index.html and http://www.arabidopsis.org/index.jsp). Because the oligonucleotide is intended for use in a diagnostic assay, a BLAST search of DNA sequences deposited in GenBank (http://www.ncbi.nlm.nih.gov/Genbank/index.html) found no homology with any known genes, thus confirming the uniqueness of the selected DNA sequence. The oligonucleotide was designed by using Primer Express (Applied Biosystems Inc., Foster City, CA) and Primer Select (DNASTAR Lasergene, WI). The DNA sequence of 75mer (75-ARD) was 5′-SS-(A)$_{10}$-GACTTTGTTCGTGGATACCCTTTCAG-

TATGCGCGAAGGTGCCATAACCGCGGTCTCTCATGG-CCTCTGGCTCAAC-3′. A 64mer (64-Pol) was created by replacing the 5′ end of 75-ARD with a DNA sequence complementary to a unique region of the human immunodeficiency virus (HIV). The sequence of 64-Pol was 5′-SS-(A)$_{10}$-TGACTTTGGGGATTGTAGGGATGCGCGAAG-GTGCCATAACCGCGGTCTCTCATGGCCTCTGGCT-3′). The 75-ARD and 64-Pol both incorporated complementary 5′ ARD-For (5′-TTGTTCGTGGATACCCTTTCAGT-3′ and Pol3097f (5′-TGACTTTGGGGATTGTAGGG-3′), respectively, and 3′ ARD-Rev (5′-AGCCAGAGGCCATGA-GAGAC-3′) primer and central [ARD-Probe (FAM-5′-TGCGCGAAGGTGCCATAACCG-3′-TAMRA)] probe binding sites. The 10-dA spacer sequence inserted between the dithiol-cap and the recognition sequence reduces both the interactions between the bases of the recognition sequence and the gold nanoparticle surface and inter-strand steric crowding as described previously (1,17). The 5′-Thiol modifier C6 S-S phosphoramidite reagent, fluroscein phosphoramidite, and other reagents required for oligonucleotide synthesis were purchased from Glen Research (Sterling, VA). All oligonucleotides were prepared with ABI 394 DNA synthesizer (Applied Biosystems Inc., Foster City, CA) using standard phosphoramidite chemistry. All experiments used

Nanopure H_2O (>18 mΩ) purified through a Barnstead NANOpure ultrapure water system.

Preparation of gold nanoparticles

Aqueous solutions of 30 nm diameter gold nanoparticles were purchased from British Bio Cell International (Cardiff, UK). Gold nanoparticles of 13 nm diameter were prepared by citrate reduction of $HAuCl_4$ (Aldrich, St Louis, MO) (18). The nanoparticles were characterized by transmission electron microscopy (TEM) performed with a Hitachi 8100 transmission electron microscope. Bright-field images of at least 250 particles deposited onto a carbon-coated 200 mesh copper grid (Ted Pella Inc., Redding, CA) were measured by using ImageTool graphics software to approximate the average particle diameter. The optical density at 520 nm was measured by using a Hewlett-Packard 8452a diode array spectrophotometer. The concentrations of the gold nanoparticles were calculated using the absorbance values in conjunction with the calculated extinction coefficient for $\varepsilon_{NP13}^{520\,nm} = 2.7 \times 10^8$ and $\varepsilon_{NP30}^{520\,nm} = 3.7 \times 10^9 cm^{-1} M^{-1}$ (19).

Preparation of DNA-modified gold nanoparticles

The $5'$ disulfide bond of the dithiol-capped oligonucleotides was cleaved with 100 mM DTT, and the oligonucleotides were purified with a NAP5 column (GE Healthcare Life Sciences, Piscataway, NJ) as described previously (20). The oligonucleotide-modified gold nanoparticle solutions were prepared by adding 2 nmol of DNA per ml of 30 nm diameter (0.1 nM) and 13 nm diameter gold (6 nM) nanoparticles. The solutions were diluted to 0.15 M NaCl, 10 mM phosphate (pH 7.4) and allowed to stand for 48 h at ambient temperature. Unconjugated oligonucleotides were removed by washing with 0.15 M NaCl, 10 mM phosphate (pH 7.4), followed by centrifugation at 10 000 r.p.m. (AM2.18 rotor) for 10 min for the 30 nm gold nanoparticles and 14 000 r.p.m. (AM2.18 rotor) for 30 min for the 13 nm gold nanoparticles. Then purification was accomplished by centrifugation at 9000 *g* for 30 min through a linear glycerol gradient of 10–30%. The thiol oligonucleotide-modified gold nanoparticles were redispersed in 0.15 M NaCl, 10 mM phosphate (pH 7.4) and the optical density at 520 nm was measured by using a HP 8452a diode array spectrophotometer.

Preparation of DNA- and antibody-modified gold nanoparticles

Sheep polyclonal antibody against HIV p24 capsid (Aalto, UK) or goat polyclonal antibody against HIV p7 nucleocapsid (AIDS Vaccine Program, Frederick, MD) were bound onto the 30 nm gold nanoparticle surface as described previously (21). The antibody-modified gold nanoparticles were bound in tandem with dithiol-capped oligonucleotides and washed to remove the reagents by using the method described, above. The functionalized gold nanoparticles were redispersed in 0.15 M NaCl, 10 mM phosphate (pH 7.4), 0.02% Tween-20.

Stability test and melting properties of oligonucleotide gold nanoparticle conjugates

Gold nanoparticles functionalized with dithiol-capped oligonucleotides were tested for their thermal stability. The oligonucleotides bound onto and desorbed from the nanoparticle surface after amplification by real-time PCR were stained with SYBR green, resolved by electrophoresis on a 4% agarose gel, and then visualized with ultraviolet light. Electronic absorption spectra of the oligonucleotide and nanoparticle solutions were measured using a HP 8453 diode array spectrophotometer equipped with a HP 89090a Peltier temperature controller. Absorbance was monitored at 520 nm from 15 s to 1 min intervals. For the melting experiment, the hybridization properties of the nanoparticle probes were studied in 0.15 M NaCl and 10 mM phosphate buffer (pH 7.0) as described previously (19). The temperature ramping range was from 25 to 75°C with an interval of 1°C and 1 min holding time for each temperature point. The melting temperature was calculated from the first derivative of the change in extinction at 520 nm, and was reported by rounding to the nearest degree.

Fluorescence-based method for determining the surface coverage of DNA–modified gold nanoparticles

To corroborate the results for the real-time PCR-based measurement of surface coverage of oligonucleotides bound onto gold nanoparticles, we used a modified fluorescence-based method described (1,20). Surface bound fluorophore (Cy3) labeled DNA was displaced by 100 mM DTT in 0.15 M NaCl, 10 mM phosphate (pH 7.4) at 40°C via an exchange reaction. With the loss of surface coverage by bound DNA, there was observable color changes associated with gold nanoparticle aggregation due to a shift in their surface plasmon resonance (22). After DTT treatment, the solutions containing displaced oligonucleotides were separated from the gold by centrifugation. Then the fluorescence of the fluorophore-labeled oligonucleotide was measured in black 96-well plates with serial diluted free fluorophore oligonucleotide by using a SpectraMax Gemini XS fluorescent plate reader (Molecular Devices, CA). Excitation and emission wavelengths (530 and 568 nm, respectively) were chosen to maximize the fluorescence intensities. In all cases the 'auto cutoff' feature of the instrument was used.

Real-time PCR-based method for determining the surface coverage of DNA-modified gold nanoparticles

Surface-bound 75-ARD DNA was quantified by real-time PCR using primers ARD-For and ARD-Rev and the fluorescence-labeled ARD-Probe. Surface-bound 64-Pol DNA was quantified by using primers Pol3097f and ARD-Rev and the fluorescent beacon probe ARD-Probe. Primers ARD-For and ARD-Rev, probe ARD-Probe, and dithiol-capped oligonucleotides 75-ARD and 64-Pol were synthesized separately to avoid adventitial cross-contamination. The TaqMan Universal Master Mix [0.025 U/μl AmpliTaq Gold DNA Polymerase, 0.2 mM each of dATP, dCTP, dGTP and dTTP, 50 mM KCl, 10 mM Tris–HCl (pH 8.3) 3.5 mM MgCl2, 10 mM EDTA and 60 nM ROX passive reference dye] was used according to the manufacturer's directions (Perkin–Elmer Applied Biosystems Inc., Foster City, CA). The cycling parameters were an initial DNA denaturation step at 95°C for 10 min followed by 40 cycles of PCR with DNA denaturation at 95°C for 15 s and primer annealing and extension at 60°C for 1 min. To document the quantity of the surface-bound DNA, the oligonucleotides 75-ARD and 64-Pol were also amplified in parallel in reactions at 10-fold serial dilutions.

DNA concentrations from these samples were used to calculate the amount of input DNA from the DNA-modified gold nanoparticles in the preparation of the standard curve. Fluorescence data were recorded with an ABI Prism 7900

sequence detection system (Applied Biosystems, Foster City, CA).

RESULTS

Thermal stability of oligonucleotides bound onto gold nanoparticles

Because the gold nanoparticle probes are ultimately intended for use in a diagnostic assay (i.e. HIV detection), it was important to determine the thermal stability of the oligonucleotides bound onto the gold nanopaticle surface. Accordingly, we measured the gel mobility and the ultraviolet (UV)-visible spectra of the DNA-modified gold nanoparticle solution as a function of temperature and oligonucleotide displacement.

We first determined whether the oligonucleotide was desorbed from the surface of the gold nanoparticle after the repeated temperature cycles used for real-time PCR. The 75-ARD and 64-Pol oligonucleotide-modified 13 and 30 nm gold nanoparticles in buffer used for the real-time PCR assay with and without dNTPs and primers were subjected to the repetitive cycles of temperature changes used for real-time PCR. After 40 cycles, the color of the solution containing the 75-ARD and 64-Pol oligonucleotide-modified 13 and 30 nm gold nanoparticles with and without dNTPs and primers remained red, indicating that the oligonucleotides were not desorbed from the nanoparticle surface. We observed this result whether the DNA-modified gold nanoparticles were in the presence or absence of primers and dNTPs that could stabilize them during thermal cycling (data not shown).

To verify that the oligonucleotides were not desorbed from the surface of the gold nanoparticle, an aliquot of the reaction mix was mixed with SYBR green and DNA loading dye, added onto a 4% agarose gel, and resolved by electrophoresis. The SYBR green stained DNA bands were visualized under UV light. For each of the oligonucleotide-modified gold nanoparticles in solution (without the added primers), the DNA mobility in the gel was consistent with it being bound onto the surface (data not shown).

When subjected to a temperature gradient commensurate with that used for annealing between the DNA bound onto the gold nanoparticle probe and target sequences in solution (range 25–75°C), the UV-visible spectra showed no evidence of particle decomposition or aggregation (Figure 2C). In solution, the DNA-modified gold nanoparticles instill a dark red color with a plasmon band centered at 520 nm. Upon addition of DTT to the DNA-modified gold nanoparticle solution, the oligonucleotides are desorbed from the gold nanoparticle surface and the denuded gold nanoparticles aggregate irreversibly. The exchange reaction is accompanied by a gradual color change from red to blue with a concomitant
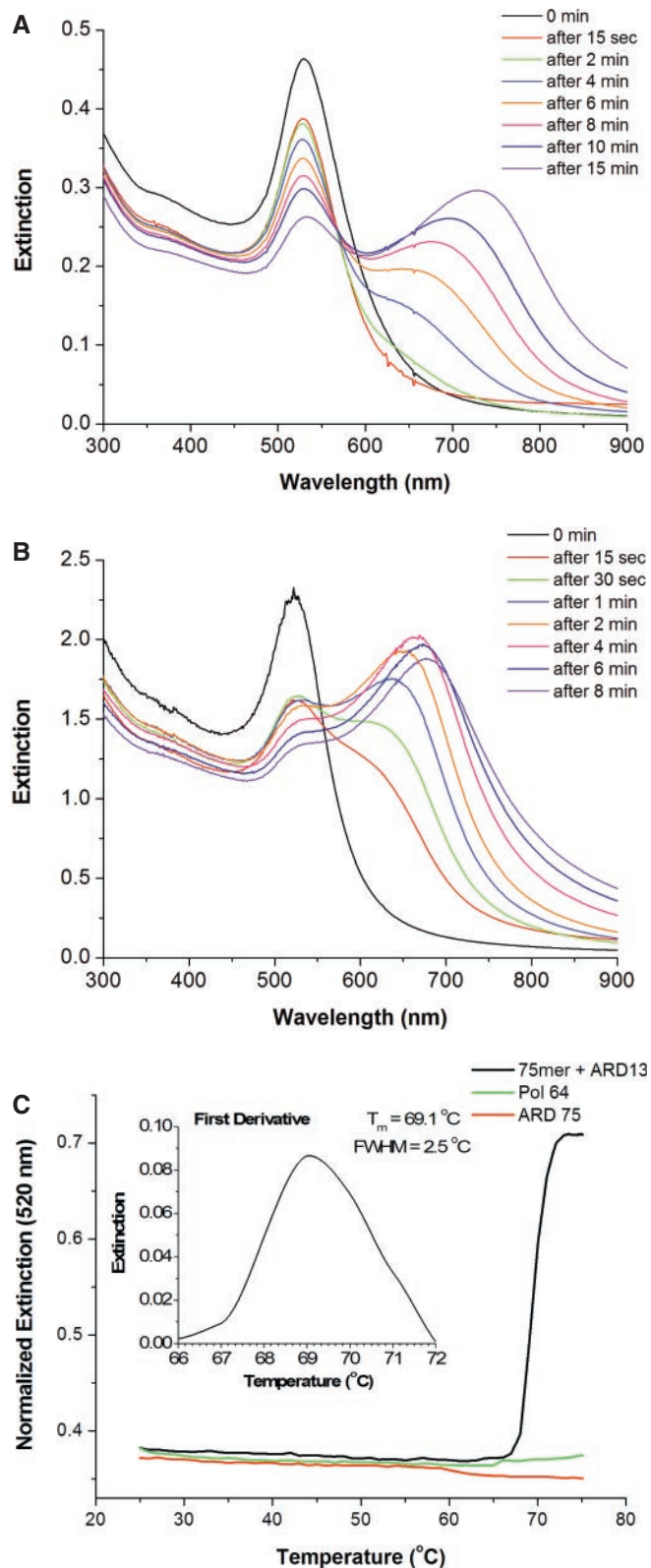
Figure 2. Time evolution of UV-vis spectra of DNA-modified gold nano-particles (**A** and **B**). Upon addition of 0.1 M DTT to the DNA-modified gold nanoparticle solution, the exchange reaction is accompanied by a gradual color change from red to blue to black and broadening of the surface plasmon band at 520 nm for 13 nm (A) and 30 nm (B) gold particles. (**C**) Melting curve of 75-ARD and 64-Pol oligonucleotide-modified 13 nm gold nanoparticles in a solution of 0.15 M NaCl, 10 mM phosphate buffer (pH 7.4); the inset shows the first derivative plot of the melting transition. Following the UV-vis spectra (green and red lines) over a temperature gradient as function of time shows that the individual DNA-modified gold nanoparticles are stable.

broadening of the 520 nm surface plasmon band (Figure 2A and B). Eventually the particles precipitate as a black mass at the bottom of the reaction vessels.

We next examined whether primers and probe could hybridize to the complementary sequences in the oligonucleotide conjugated gold nanoparticle surface. For a mix of the 75-ARD oligonucleotide-modified gold nanoparticle and the ARD-Rev primer (ARD13), which is complementary to a 20 nt span closest to the 5′-thiol group bound to the nanoparticle surface, yielded a sharp melting transition at 69.1°C; a value consistent with the calculated melting temperature (Figure 2C). This result, and the results for the other primer (ARD-For) and probe (ARD-Probe) for both the 75-ARD and 64-Pol oligonucleotide-modified gold nanoparticles (data not shown), demonstrated appropriate annealing of primers and probe to the complementary sequences of the oligonucleotide-modified gold nanoparticles. Thus, the oligonucleotide bound onto the gold nanoparticle surface is a suitable target for amplification by real-time PCR.

Real-time PCR-based measurement of surface coverage of oligonucleotides bound onto gold nanoparticles

Real-time PCR was used to determine the surface coverage of thiol-capped oligonucleotides bound onto gold nanoparticles. Because real-time PCR measurements in the context of DNA surface coverage require the DNA-modified gold nanoparticle solution to go through repetitive cycles of changing temperature, it was important to determine whether the gold nanoparticles affected the fidelity of the real-time PCR. For real-time PCR, the 3′ quencher dye (TAMRA) absorbs the fluorescence emission of the 5′ reporter dye (FAM) on the intact probe until such time that the 5′ exonuclease activity of the *Taq* polymerase separates the FAM from the TAMRA, which produces a fluorescence emission.

Gold nanoparticles absorb a significant amount of light between 200 and 530 nm; thus, their presence in solution could effect fluorescence measurements by acting as a filter and diminishing the available excitation energy and the intensity of emitted radiation. Significantly, the gold surface plasmon band at 520 nm matches the emission maximum of fluorescein. Accordingly, we quantified the oligonucleotide target by real-time PCR in the absence and presence of gold nanoparticles. The FAM fluorescence signal intensity and the quantity of target DNA in the reaction was the same whether gold nanoparticles were in the reaction mix or not (data not shown). Thus, the oligonucleotide is an apt target for robust amplification by PCR, regardless of whether it is bound onto or desorbed from the gold nanoparticle surface.

To determine the surface coverage of dithiol-capped oligonucleotide bound onto gold nanoparticles, solutions containing the 64-Pol and 75-ARD oligonucleotide-modified 13 and 30 nm gold nanoparticles were reduced by serial 10-fold dilutions with water. The 64-Pol and 75-ARD oligonucleotide template controls were diluted in parallel and used to generate a standard curve. Figure 3 shows representative amplification profiles and standard curves for a set of 75-ARD standards (Figure 3A) and for 75-ARD bound onto 30 and 13 nm gold nanoparticles (Figure 3B and C, respectively). The 64-Pol and 75-ARD standard curves were used to quantify the amount of oligonucleotide in the sample and then calculate the surface
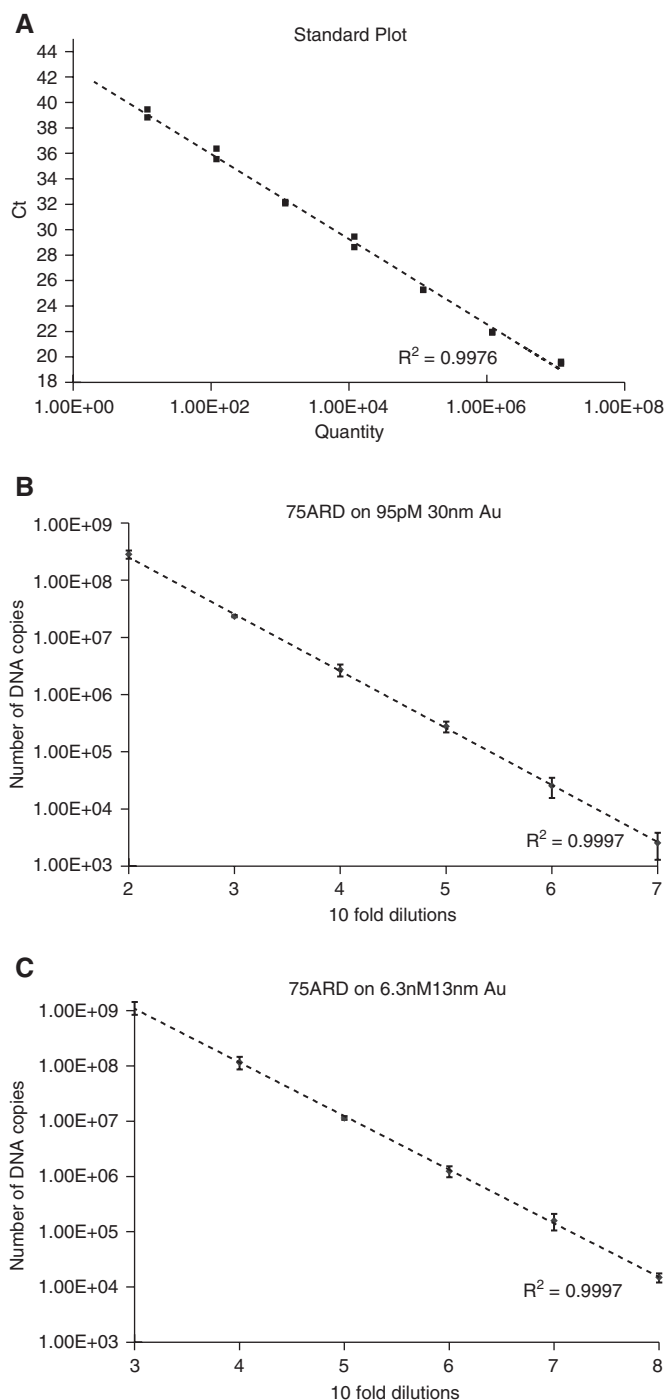
Figure 3. Precision and accuracy of real-time PCR. 75-ARD amplification profiles and standard curves generated for the oligonucleotide alone (**A**) and bound onto 13 nm gold nanoparticle (**B**) and the 30 nm gold nanoparticle (**C**). Levels of 75-ARD were quantified on an Applied BioSystems PRISM 7900HT Sequence Detection System.

coverage of the 64-Pol and 75-ARD 5′-thiol oligonucleotides bound onto the gold nanoparticle surface. All curves had excellent correlation coefficients (>0.997).

As shown in Table 1, the surface coverage of 64-Pol and 75-ARD 5′-thiol oligonucleotides bound onto 13 nm gold nanoparticles was on average 93 ± 21 and 87 ± 12 DNA

Table 1. Surface coverage of oligonucleotides bound onto 13 and 30 nm gold nanoparticles determined by the real-time PCR-based method

Gold nanoparticles	Oligo nucleotide	Antibody conjugates (1.5 µg/ml)	Mean coverage of DNA molecules/ particle	pmol/cm^2
13 nm	64-Pol	—	93 ± 21	29.2 ± 6.6
	75-ARD	—	87 ± 12	27.2 ± 3.8
30 nm	64-Pol	—	228 ± 27	13.4 ± 1.6
	75-ARD	—	220 ± 23	13.0 ± 1.4
		anti-p7	149 ± 48	8.7 ± 2.8
		anti-p24	180 ± 51	10.6 ± 2.9

The values for the mean coverage of DNA bound onto gold nanoparticles are the results for multiple measurements ($n = 5$) using multiple batches ($n = 3$) of gold nanoparticles.

strands per particle for an estimated 29.2 ± 6.6 pmol/cm^2 and 27.2 ± 3.8 pmol/cm^2, respectively. For 30 nm gold nanoparticles, the surface coverage of 64-Pol and 75-ARD 5′-thiol oligonucleotides was on average 228 ± 27 and 220 ± 23 DNA strands per particle for an estimated 13.4 ± 1.6 pmol/cm^2 and 13.0 ± 1.4 pmol/cm^2, respectively. All values represent five independent real-time PCR measurements for each of three different batches of 13 and 30 nm gold nanoparticles. When antibodies are conjugated with gold nanoparticles a reduced surface coverage of 5′-thiol oligonucleotides is observed; the extent of reduction in the amount of surface coverage by DNA was associated with the concentration of bound antibody. The average of the recorded values for oligonucleotides bound onto the gold nanoparticle surface in the presence of bound antibodies against HIV p24 and p7 were similar.

Fluorescence-based measurement of surface coverage of oligonucleotides bound onto gold nanoparticles

Surface coverage studies using the fluorescence-based method was performed by thoroughly washing away unbound oligonucleotides, followed by removal of fluorophore-labeled oligonucleotides from the gold nanoparticle surface via an exchange reaction with DDT, elimination of the gold nanoparticles from the solution, and quantification of the oligonucleotide concentration by using fluorescence spectrophotometry. Separation of fluorophore-labeled oligonucleotides from the gold nanoparticle is necessary because the signal for surface-bound fluorescein-modified oligonucleotides (530 nm excitation, 586 nm emission) is quenched by fluorescence resonance energy transfer; gold nanoparticles in solution diminish the available excitation energy by absorbing light between 200 and 530 nm. (16)

In the absence of affixed antibody, the average surface coverage of the fluorophore-modified 75-ARD thiol-oligonucleotide bound onto the 30 nm gold nanoparticle was 11.7 ± 0.7 pmol/cm^2 for an estimated 199 ± 12 DNA strands per particle. (See Supplementary Data). By comparison, the average surface coverage of the 75-ARD 5′-thiol oligonucleotide measured by the real-time PCR method was 13.4 ± 1.5 pmol/cm^2 for an estimated 220 ± 23 DNA strands per 30 nm gold nanoparticle. Thus, the fluorescence- and real-time PCR-based measurements of surface coverage of oligonucleotides bound onto gold nanoparticles were quantitatively similar. The final surface coverage for gold

nanoparticles decreased with increasing concentrations of antibody, demonstrating a linear relationship between antibody concentration and DNA strand surface coverage measurements (data not shown).

CONCLUSION

We have developed a real-time PCR-based method for determining the surface coverage of thiol-capped oligonucleotides bound onto gold nanoparticles in the presence and absence of antibody. The average oligonucleotide surface coverage of 5′-thiol-modified 64mer (64-Pol) and 75mer (75-ARD) oligonucleotides on 13 or 30 nm gold nanoparticles was ∼30 and 13 pmol/cm^2, respectively. For 13 nm gold nanoparticles, this corresponds to ∼93 ± 21 thiol-bound 64mer strands and 87 ± 12 75mer strands per particle. For 30 nm gold nanoparticles, this corresponds to ∼228 ± 27 thiol-bound 64-Pol DNA strands and 220 ± 23 thiol-bound 75-ARD DNA strands per particle. When antibodies are conjugated onto the gold nanoparticle surface in tandem, there was a linear relationship between antibody concentration and DNA strand surface coverage measurements ($r^2 = 0.9$). A fluorescence-based method for determining the surface coverage of oligonucleotides bound onto the gold nanoparticle surface gave comparable results (1) (Supplementary Data).

Unlike the immobilization of oligonucleotides onto planar gold surfaces, we did not find a significant reduction in surface coverage of gold nanoparticles with increased oligonucleotide length (23). The high surface coverage of oligonucleotides bound onto the gold nanoparticle is attributable to the high curvature of the nanoparticle surface that helps to overcome inter-strand steric interference (1). Spacer sequences on the nanoparticle surface can extend the bound oligonucleotides away from the surface and from their neighbors. In addition to lessening the extent to which the oligonuicleotides crowd each other, the spacers move the oligonucleotide further away from the surface to allow better interaction with the target, and therefore improve hybridization efficiency (1,17).

The real-time PCR-based method for determining the surface coverage of thiol-capped oligonucleotides bound onto gold nanoparticles requires complementary binding sites in the oligonucleotides that are accessible for primer and probe annealing, primer extension, and 5′-exonuclease cleavage of the probe. The minimum oligonucleotide (amplicon) length required for robust amplification by real-time PCR (∼60mer) is a limitation, however. The increased stability of DNA duplexes formed with minor groove binder-oligonucleotide conjugate probes and complementary DNA allows the use of shorter probes for real-time PCR, and therefore shorter oligonucleotides (∼50mer) bound onto the gold nanoparticle surface (23). Related methods that use DNA ligase are being adapted for quantification of even shorter strands (∼20mer; E.-Y. Kim, J. Stanton, K. J. Kunstman and S. M. Wolinsky, unpublished data).

Unlike the fluorescence-based method for determining surface coverage, the real-time PCR-based method does not require the synthesis of a model system with fluorophore labels, but rather allows for direct measurement of the surface coverage on the unlabeled probes. Because the fluorescence emission for real-time PCR is produced after the 5′ exonuclease activity of the Taq polymerase separates the FAM from the

TAMRA, the fluorescence signal is not quenched as a result of fluorescence resonance energy transfer to the gold nanoparticle. Collisions of the fluorophore against the gold nanoparticle (i.e. dynamic quenching) did not add to the quenching of fluorescence in the real-time PCR assay. Although the gold nanoparticles absorb a significant amount of light at the emission maximum of fluorescein, their presence in the reaction mixture did not significantly affect the intensity of emitted radiation in these experiments.

The real-time PCR-based method offers a rapid, simple approach to elucidating the surface coverage and hybridization efficiency of thiol-capped oligonucleotides bound onto gold nanoparticles. It can be used to explore the effects of oligonucleotide content and length, co-absorbed molecules (e.g. antibody), oligonucleotide spacer sequence, and the influence of solution concentration on probe surface coverage and hybridization efficiency. It also allows independent verification of other nanoparticle-based techniques that use oligonucleotide probes with high specificity and high binding affinity to target unique polynucleotide sequences. When combined with pairs of antibodies against different epitopes on the same protein in the bio-barcode amplification assay, the real-time PCR-based method can quantify amounts of protein that are below the limit of detection by standard immunoassays. The method has important implications for understanding the structure and function of oligonucleotides immobilized onto surfaces and for optimizing the sensitivity of oligonucleotide-modified gold nanoparticle-based detection methods.

SUPPLEMENTARY DATA

Supplementary Data are available at NAR Online.

ACKNOWLEDGEMENTS

REFERENCES

1. Demers,L.M., Mirkin,C.A., Mucic,R.C., Reynolds,R.A.III, Letsinger,R.L., Elghanian,R. and Viswanadham,G. (2000) A fluorescence-based method for determining the surface coverage and hybridization efficiency of thiol-capped oligonucleotides bound to gold thin films and nanoparticles. *Anal. Chem.*, **72**, 5535–5541.
2. Festag,G., Steinbruck,A., Wolff,A., Csaki,A., Moller,R. and Fritzsche,W. (2005) Optimization of gold nanoparticle-based DNA detection for microarrays. *J. Fluoresc.*, **15**, 161–170.
3. Liang,R.Q., Li,W., Li,Y., Tan,C.Y., Li,J.X., Jin,Y.X. and Ruan,K.C. (2005) An oligonucleotide microarray for microRNA expression analysis based on labeling RNA with quantum dot and nanogold probe. *Nucleic Acids Res.*, **33**, e17.
4. Sato,K., Hosokawa,K. and Maeda,M. (2005) Non-cross-linking gold nanoparticle aggregation as a detection method for single-base substitutions. *Nucleic Acids Res.*, **33**, e4.
5. Huber,M., Wei,T.F., Muller,U.R., Lefebvre,P.A., Marla,S.S. and Bao,Y.P. (2004) Gold nanoparticle probe-based gene expression analysis with unamplified total human RNA. *Nucleic Acids Res.*, **32**, e137.
6. Nicewarner Pena,S.R., Raina,S., Goodrich,G.P., Fedoroff,N.V. and Keating,C.D. (2002) Hybridization and enzymatic extension of au nanoparticle-bound oligonucleotides. *J. Am. Chem. Soc.*, **124**, 7314–7323.
7. Daniel,M.C. and Astruc,D. (2004) Gold nanoparticles: assembly, supramolecular chemistry, quantum-size-related properties, and applications toward biology, catalysis, and nanotechnology. *Chem Rev.*, **104**, 293–346.
8. Foultier,B., Moreno-Hagelsieb,L., Flandre,D. and Remacle,J. (2005) Comparison of DNA detection methods using nanoparticles and silver enhancement. *IEE Proceedings-Nanobiotechnology*, **152**, 3–12.
9. Park,S.J., Lazarides,A.A., Mirkin,C.A., Brazis,P.W., Kannewurf,C.R. and Letsinger,R.L. (2000) The electrical properties of gold nanoparticle assemblies linked by DNA. *Angewandte Chemie.*, **39**, 3845–3848.
10. Patolsky,F., Weizmann,Y., Lioubashevski,O. and Willner,I. (2002) Au-nanoparticle nanowires based on DNA and polylysine templates. *Angew Chem. Int. Ed. Engl.*, **41**, 2323–2327.
11. Moller,R., Csaki,A., Kohler,J.M. and Fritzsche,W. (2000) DNA probes on chip surfaces studied by scanning force microscopy using specific binding of colloidal gold. *Nucleic Acids Res.*, **28**, E91.
12. Mirkin,C.A., Letsinger,R.L., Mucic,R.C. and Storhoff,J.J. (1996) A DNA-based method for rationally assembling nanoparticles into macroscopic materials. *Nature*, **382**, 607–609.
13. Kohli,P., Harrell,C.C., Cao,Z., Gasparac,R., Tan,W. and Martin,C.R. (2004) DNA-functionalized nanotube membranes with single-base mismatch selectivity. *Science*, **305**, 984–986.
14. Steel,A.B., Herne,T.M. and Tarlov,M.J. (1998) Electrochemical quantitation of DNA immobilized on gold. *Anal. Chem.*, **70**, 4670–4677.
15. Peterlinz,K.A., Georgiadis,R.M., Herne,T.M. and Tarlov,M.J. (1997) Observation of hybridization and dehybridization of thiol-tethered DNA using two-color surface plasmon resonance spectroscopy. *J. Am. Chem. Soc.*, **119**, 3401–3402.
16. Dubertret,B., Calame,M. and Libchaber,A.J. (2001) Single-mismatch detection using gold-quenched fluorescent oligonucleotides. *Nat. Biotechnol.*, **19**, 365–370.
17. Storhoff,J.J., Elghanian,R., Mirkin,C.A. and Letsinger,R.L. (2002) Sequence-dependent stability of DNA-modified gold nanoparticles. *Langmuir*, **18**, 6666–6670.
18. Grabar,K.C., Freeman,G.R., Hommer,M.B. and Natan,M.J. (1995) Preparation and characterization of Au colloid monolayers. *Anal. Chem.*, **67**, 735–743.
19. Jin,R., Wu,G., Li,Z., Mirkin,C.A. and Schatz,G.C. (2003) What controls the melting properties of DNA-linked gold nanoparticle assemblies? *J. Am. Chem. Soc.*, **125**, 1643–1654.
20. Li,Z., Jin,R., Mirkin,C.A. and Letsinger,R.L. (2002) Multiple thiol-anchor capped DNA-gold nanoparticle conjugates. *Nucleic Acids Res.*, **30**, 1558–1562.
21. Nam,J.M., Thaxton,C.S. and Mirkin,C.A. (2003) Nanoparticle-based bio-bar codes for the ultrasensitive detection of proteins. *Science*, **301**, 1884–1886.
22. Chowdhury,M.H., Julian,A.M., Coates,C.J. and Cote,G.L. (2004) Detection of differences in oligonucleotide-influenced aggregation of colloidal gold nanoparticles using absorption spectroscopy. *J. Biomed. Opt.*, **9**, 1347–1357.
23. Kutyavin,I.V., Afonina,I.A., Mills,A., Gorn,V.V., Lukhtanov,E.A., Belousov,E.S., Singer,M.J., Walburger,D.K., Lokhov,S.G., Gall,A.A. *et al.* (2000) 3′-minor groove binder-DNA probes increase sequence specificity at PCR extension temperatures. *Nucleic Acids Res.*, **28**, 655–661.